



Morpholine-based RGD-cyclopentapeptides as $\alpha_v\beta_3/\alpha_v\beta_5$ integrin ligands: Role of configuration towards receptor binding affinity

Nicoletta Cini^{a,b}, Andrea Trabocchi^a, Gloria Menchi^{a,c}, Anna Bottoncetti^b, Silvia Raspanti^{b,c}, Alberto Pupi^{b,c}, Antonio Guarna^{a,c,*}

^aDipartimento di Chimica Organica "Ugo Schiff", Università degli Studi di Firenze, Polo Scientifico e Tecnologico, Via della Lastruccia 13, I-50019 Sesto Fiorentino (FI), Italy

^bDipartimento di Fisiopatologia Clinica, Unità di Medicina Nucleare, Università degli Studi di Firenze, Viale Pieraccini 6, I-50134 Firenze, Italy

^cCentro Interdipartimentale per lo Sviluppo Preclinico dell'Imaging Molecolare (CISPIM), Università degli Studi di Firenze, Viale Pieraccini 6, I-50134 Firenze, Italy

ARTICLE INFO

Article history:

Received 2 September 2008

Revised 5 January 2009

Accepted 7 January 2009

Available online 13 January 2009

Keywords:

Peptide

Peptidomimetic

Conformational analysis

NMR

ABSTRACT

Two c[RGDfX] cyclopeptides, having either L- or D-morpholine-3-COOH (Mor) as the X amino acid were developed as ligands for $\alpha_v\beta_3/\alpha_v\beta_5$ integrins. Biological assays showed only D-Mor-containing cyclopentapeptide capable to bind $\alpha_v\beta_3$ integrin with a low nanomolar affinity according to a two-site model, thus revealing a connection between the configuration of Mor and the preferred binding to $\alpha_v\beta_3$ integrin. Conformational analysis showed different structural preferences for the two peptides induced by the two enantiomeric cyclic amino acids, suggesting a role of the stereochemistry of Mor on the overall peptide conformation and on the presentation of the pharmacophoric Arg and Asp side chains.

© 2009 Elsevier Ltd. All rights reserved.

1. Introduction

Integrins are a class of cellular receptors known to bind extracellular matrix proteins, and therefore mediate cell adhesion events. The integrin receptors constitute a family of proteins with structural characteristics of non-covalent heterodimeric glycoprotein complexes formed of α and β subunits.¹ The vitronectin receptor is known to refer to three different integrins, named $\alpha_v\beta_1$, $\alpha_v\beta_3$ and $\alpha_v\beta_5$. While $\alpha_v\beta_3$ binds a large variety of ligands, $\alpha_v\beta_5$ binds exclusively vitronectin. One important recognition site in a ligand for many integrins is the arginine–glycine–aspartic acid (RGD) tripeptide sequence,² which is found in all peptide-based ligands identified for the vitronectin receptor integrins. Among the RGD-dependent integrins, the $\alpha_v\beta_3$ and $\alpha_v\beta_5$ receptors have received increasing attention as therapeutic targets as they are expressed in various cell types and are involved in osteoporosis, arthritis, retinopathy, and tumour-related processes.³ The RGD recognition site can be mimicked by polypeptides that contain the RGD sequence, and the specificity of the inhibition can be modulated by the sequence and structure of such peptides, so as to target specific integrins. $\alpha_v\beta_3$ antagonists, including RGD-containing peptides, have been successfully applied as inhibitors of blood vessel development and tumour growth.⁴ Also, the role of $\alpha_v\beta_3$ integrin in processes that involve tumour growth and metas-

tasis has been demonstrated, as its expression is up-regulated on metastatic melanoma⁵ and late stage glioblastoma.⁶ Recent studies have also confirmed the implication of the $\alpha_v\beta_5$ integrin in angiogenesis, possibly through a distinct signalling pathway, activated by different growth factors, such as VEGF.⁴ During last decade the cyclic peptide c[RGDfV] as a selective ligand for the $\alpha_v\beta_3$ integrin, was developed by Kessler and co-workers through a 'spatial screening' of libraries of c[RGDYX] cyclopentapeptides containing the RGD sequence, demonstrating the influence of residues X and Y on the $\alpha_v\beta_3$ inhibition.⁷ In particular, high inhibition activity was found for compounds having at position 4, corresponding to the (i + 1) position of a type-II' β -turn, an aromatic hydrophobic D-amino acid, such as D-Phe or D-Trp (or, alternatively, a D-serine) or a glycine. Also, a more variable substitution pattern for the X amino acid was ascertained not to have a great influence on the $\alpha_v\beta_3$ inhibition, although a relatively lower activity was generally found for cyclopentapeptides displaying D-amino acids at such position of the sequence. As a result of these SAR analyses, many different cyclic RGD-containing peptides have been reported by replacement of the central D-Phe-Val dipeptidic sequence with different turn mimetics and sugar amino acids, with the aim of increasing the conformational constraint of the RGD sequence.⁸ In particular, the N-methylated derivative c[RGDf(Me)Val] (Cilengitide, EMD121974),^{8b} which is actually being examined in clinical phase II as an angiogenesis inhibitor, resulted in significantly higher binding affinity with respect to the parent c[RGDfV] peptide.

* Corresponding author. Tel.: +39 055 4573538; fax: +39 055 4573569.

E-mail address: antonio.guarna@unifi.it (A. Guarna).

In continuation of our research focused on the development of morpholine-based heterocycles for peptidomimetic chemistry,⁹ we recently reported a new efficient method for the preparation of *N*-Fmoc-morpholine-3-carboxylic acid starting from serine, and the introduction in a model peptide by means of solid-phase peptide synthesis (SPPS) was also described.¹⁰ With the aim of exploring the possibility of using this secondary amino acid in peptidomimetic chemistry, we devised new RGD-based peptidomimetics containing the morpholine nucleus as a replacement of *N*-methyl-valine of Cilengitide as potential integrin ligands, and also we were interested in understanding the effect of the configuration of such amino acid towards receptor affinity and selectivity, as a result of different conformational preferences of cyclopeptides containing the two enantiomeric cyclic amino acids. Thus, both c[RGDfX] cyclopeptides **1** and **2**, containing either *L*- or *D*-morpholine-3-carboxylic acid, respectively (Fig. 1), were synthesized on solid-phase and assayed *in vitro* towards $\alpha_v\beta_3$ and $\alpha_v\beta_5$ integrins. Moreover, the conformational analysis by NMR was assessed so as to relate differences in the biological affinity to different conformational preferences induced by the shift of configuration of the two enantiomeric cyclic amino acids. Due to the hydrophilic character of the title cyclopeptides, the conformational analysis by NMR was carried out in DMSO-*d*₆,⁷ thus investigating both hydrogen-bonding by variable temperature 1D experiments, and the 3D structural organisation by TOCSY and ROESY analysis.

2. Results and discussion

2.1. Synthesis

Fmoc-protected *L*- and *D*-Mor were obtained from dimethoxyacetaldehyde and *L*- or *D*-serine methyl ester, respectively, through a short and practical synthetic route consisting of a five-step process based on reductive amination, Fmoc protection of the amine group, intramolecular acetalization and concomitant elimination of the anomeric methoxy substituent, followed by double bond hydrogenation of the resulting oxazine, and final acidic ester hydrolysis.¹⁰ The linear peptide sequences were prepared on solid-phase starting from glycine bound to acid-labile 2-Cl-trityl resin (Scheme 1).

Amino acid couplings were carried out using DIPC/HOBt as COOH activators, and the prosecution of the reaction was monitored with 1% bromophenol blue (BB) solution as internal indicator.¹¹ Coupling of Mor and of Asp were achieved with complete

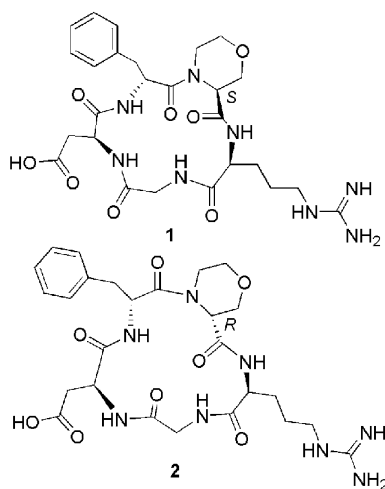


Figure 1. c[RGDfMor] cyclopeptides **1** and **2** containing *L*-Mor and *D*-Mor, respectively.

conversion using TBTU/DIPEA as the activating mixture in DMF after two days and overnight reacting, respectively. The side-chain protected linear peptide was cleaved from the resin with 1% TFA in CH₂Cl₂, and successively allowed to cyclize in diluted DMF solution using TBTU as the COOH activator. After purification of the cyclic protected peptide by standard chromatography, pure compound was achieved by deprotection of Arg and Asp side chains with 95% TFA and TIS/H₂O as scavengers, followed by HPLC purification and elution of the collected fractions over an ion-exchange resin to give the corresponding pure peptide as the hydrochloride salt.

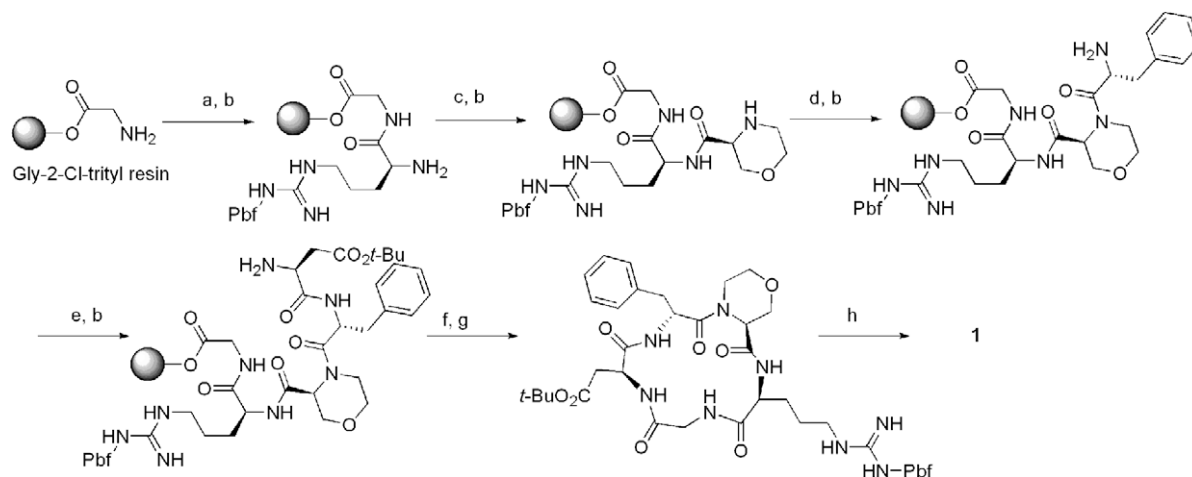
2.2. Biological assay

The ability of the tested compounds **1** and **2** to compete with [¹²⁵I]-echistatin for binding to the isolated, purified $\alpha_v\beta_3$ and $\alpha_v\beta_5$ integrins originated from human placenta^{12,13} was evaluated in solid-phase receptor assays.^{4b,14} Competition studies were carried out using a fixed concentration of the radioligand (0.05 nM and 0.1 nM for $\alpha_v\beta_3$ and $\alpha_v\beta_5$ receptors, respectively) and a range of concentrations between 100 μ M and 0.01 nM of the tested molecules. The IC₅₀ \pm SEM values (nM) were calculated as the concentration of compound required for 50% inhibition of radioligand binding, as estimated by the GraphPad Prism program, and the results are reported in Table 1.

Interestingly, the IC₅₀ values obtained showed similar binding affinity of compounds **1** and **2** towards $\alpha_v\beta_5$ receptor, whereas peptide **2** proved to bind to $\alpha_v\beta_3$ integrin with significant higher affinity with respect to diastereomeric peptide **1**. Such evidence of *D*-Mor-containing peptide **2** as a better ligand for $\alpha_v\beta_3$ integrin suggested the shift of configuration from *L*- to *D*-Mor to induce a significant conformational variation towards the optimal presentation of the pharmacophoric groups of the ligand. Moreover, the $\alpha_v\beta_3$ inhibition curve of compound **2** showed Hill slope values different from unity, indicating the binding curve to be better described by a two-sites model (Fig. 2), as a consequence of binding of **2** with two states of the integrin, in agreement with other ligands already described in the literature.¹⁵ Thus, the analysis of the data with non-linear fitting indicated cyclopeptide **2** to bind to $\alpha_v\beta_3$ receptor according to a two-site binding model. As a possible explanation, such effect could be due to different affinity conformational states that can be assumed by the integrins.^{16,17} The transition from low-affinity to high-affinity conformation has been described to be induced by natural ligands,¹⁸ and also by most ligand-mimetic antagonists.¹⁹ Moreover, it was reported that some antagonists, such as the disintegrin echistatin, bind to the active and inactive forms with similar affinity, whereas others bind to the active form with higher affinity than to the inactive form.²⁰ The data obtained suggest a similar binding behaviour for compound **2**, however further studies need to be conducted to clarify its binding properties. More importantly, the affinity data proved that the introduction of *D*-Mor in the cyclic peptide **2** does not destroy its affinity for the integrins, and induce important variations in the Arg-Gly-Asp conformation with respect to the corresponding *L*-Mor-containing peptide **1**. Interestingly, in this case, in contrast to Kessler's observation, the presence at the X position of the peptide c[RGDfX] of a *D*-amino acid mimetic significantly increases the integrin affinity compared to isomer **1**, which experiences a *L*-residue at the position X.

2.3. Conformational analysis

Conformational analysis of cyclopeptides **1** and **2** was carried out to assess the structural determinants leading to differences in binding activity towards $\alpha_v\beta_3$. Diluted DMSO-*d*₆ solutions of **1** and **2** were used for the NMR analysis in order to prevent aggregation. TOCSY, ROESY and variable temperature ¹H NMR experiments



Scheme 1. Representative synthesis of compound **1**, containing L-Mor. Reagents and conditions: (a) Fmoc-Arg(Pbf)-OH, DIPC/HOBt, BB, DMF, rt, overnight; (b) 30% piperidine in DMF, rt, 30 min; (c) Fmoc-L-Mor-OH, TBTU, DIPEA, DMF, rt, 2 d; (d) Fmoc-D-Phe-OH, DIPC/HOBt, BB, DMF, rt, overnight; (e) Fmoc-Asp(t-Bu)-OH, TBTU, DIPEA, DMF, rt, overnight; (f) 1% TFA, CH₂Cl₂, rt, 10 × 2 min; (g) TBTU, DIPEA, DMF, rt, 24 h; (h) 95% TFA, 2.5% H₂O, 2.5% TIS, rt, 2 h.

Table 1

Inhibition of [¹²⁵I]-echistatin specific binding to purified human integrin proteins $\alpha_v\beta_3$ and $\alpha_v\beta_5$ by compounds **1** and **2**

Compound	$\alpha_v\beta_5$		$\alpha_v\beta_3$		Two-site model, $\alpha_v\beta_3$			
	IC ₅₀ ^a	Hill slope	IC ₅₀ ^a	Hill slope	IC _{50h} ^a	% _h	IC _{50l} ^a	% _l
1	15.1 ± 2.3	−0.80	157 ± 0.9	−0.81				
2	21.0 ± 2.1	−0.83	32.6 ± 7.0	−0.56	6.5 ± 2.0	55.5	458 ± 191	44.5
Echistatin	0.29 ± 0.02 ^b		0.29 ± 0.08 ^b					
EMD121974	0.13 ± 0.01 ^b		18.9 ± 3.1 ^b					
ST1646	0.9 ± 0.1 ^c		5.64 ± 0.40 ^c					

^a IC₅₀ values (expressed in nM) represent the mean ± SEM of three experiments performed in triplicate. IC_{50h} and IC_{50l} correspond to IC₅₀ in the receptor high- and low-affinity states, respectively; %_h and %_l represent the proportions of high- and low-affinity states of the receptor.

^b For literature values, see Ref. 8f.

^c This assay. For literature values, see Refs. 8d,f.

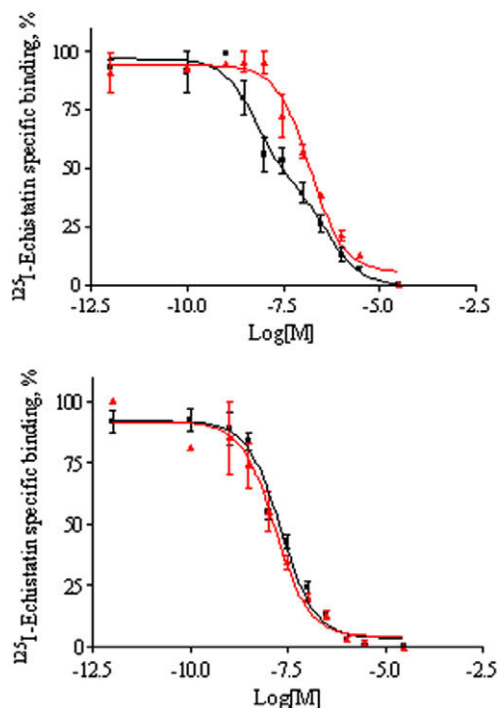


Figure 2. Inhibition of [¹²⁵I]-echistatin specific binding to purified human integrin proteins $\alpha_v\beta_3$ (top) and $\alpha_v\beta_5$ (bottom) by compounds **1** (red) and **2** (black). Each point represents the mean value ± SEM of three experiments performed in triplicate.

were carried out for the NMR analysis. Peptide **1**, having the L-Mor nucleus resulted in a unique rotamer at the D-Phe-L-Mor amide bond, whose *trans*-configuration was established by a ROESY cross peak between L-Mor H-5 and D-Phe H- α . Variable temperature experiments showed low temperature coefficients for D-Phe NH and Asp NH, suggesting such protons to be involved in intramolecular hydrogen-bonds. The chemical shift of Asp NH indicated such proton to be solvent exposed to some extent, indicating the existence of a conformational equilibrium between hydrogen-bonded and non-hydrogen-bonded states for this amide proton (Table 2).

Table 2

Chemical shifts and temperature-dependent ¹H NMR data for amide protons of peptides **1** and **2**^a

Compound	NH	δ	$\Delta\delta/\Delta T$
1	Arg	6.51	−0.5
	Gly	6.68	−5.5
	Asp	8.35	2.8
	D-Phe	7.51	−2.0
	L-Mor	7.51	−2.0
2	Arg	8.06	− ^b
	Gly	8.59	−8.5
	Asp	7.53	−2.9
	D-Phe	8.76	−5.7
	L-Mor	8.76	−5.7

^a ¹H NMR spectra for determining temperature coefficients were obtained at 298–323 K with increments of 5 K. δ values are reported in ppm and $\Delta\delta/\Delta T$ coefficients in ppb/K.

^b Broadening of Arg NH signal due to exchange phenomenon complicated the interpretation of NMR data, including the evaluation of the corresponding $\Delta\delta/\Delta T$ coefficient.

Also, the positive value for the temperature coefficient of Asp NH suggested the intramolecular hydrogen-bonded state to be stabilized upon increasing the temperature. This evidence confirmed the hypothesis of the existence of equilibrating conformations for peptide **1**, each stabilized by an intramolecular hydrogen-bond with either Asp or D-Phe amide protons. ROESY data provided additional informations about the conformational preferences of **1** in solution (Fig. 3). Specifically, ROESY peaks between D-Phe NH and Asp H- α and between Gly NH and Arg H- α supported the existence of equilibrating intramolecular hydrogen-bonds experienced by Asp and D-Phe amide protons, respectively.

Cyclopeptide **2** displayed a different conformational profile with respect to peptide **1**, suggesting the configuration of morpholine-3-carboxylic acid to play a role in the nucleation of the overall structure. ^1H NMR data of diluted DMSO- d_6 solution of **2** showed a single set of signals, attributable to the existence of a single rotamer, in analogy with **1**. The absence of any relevant ROESY cross peak between D-Phe H- α and both H-5 and H-3, and the accidental isochrony of D-Phe H- α and H-3 allowed to assign a *cis*-geometry at the D-Phe-D-Mor amide bond. Variable temperature experiments showed high $\Delta\delta/\Delta T$ coefficients for Gly and D-Phe amide protons (Table 2), indicating such protons to be solvent-exposed and not to participate in any relevant intramolecular hydrogen-bond. Conversely, a $\Delta\delta/\Delta T$ value of -2.9 and a chemical shift of 7.53 ppm suggested the existence of a hydrogen-bonded state for Asp NH. The ROESY analysis of **2** showed similar sequential ROESY peaks as observed for **1**, and specifically between D-Phe NH and Asp H- α and between Gly NH and Arg H- α , which, in conjunction with the existence of a *cis*-configuration at the D-Phe-D-Mor peptide bond, allowed to propose the preferred conformation of **2** in solution, as shown in Figure 3, bottom. The existence of a stable hydrogen-bonded structure, suggested D-Mor nucleating a more compact structure, ultimately resulting in a more rigid conformation with respect to the diastereomeric peptide **1**.

Molecular modelling calculations were carried out to give more insight about the conformational preferences of peptides **1** and **2**. Specifically, the conformational preferences of compounds **1** and **2** were investigated by molecular mechanics calculations within the framework of Macromodel v6.5,²¹ using Amber²² as a force field and the implicit water GB/SA solvation model of Still et al.²³ Monte Carlo energy minimization (MCEM)²⁴ conformational searches of the peptide analogues containing methyl groups in-

stead of the Arg and Asp side chains were performed as the first step and using conformational constraints according to ROESY data. Conformational analysis of **1** resulted in two families of conformers stabilized by intramolecular hydrogen-bonds. Specifically, the group comprising the global minimum conformer displayed a hydrogen-bond between Asp NH and Arg C=O ($E_{\text{rel}} = 0$ kcal/mol; Fig. 4, top left), and the second group showed a doubly hydrogen-bonded structure between Gly NH and D-Phe C=O, and between D-Phe NH and Gly C=O ($E_{\text{rel}} = +1.6$ kcal/mol; Fig. 4, top right). Also, the second conformation displayed the Mor carbonyl group oriented in the less stable equatorial position, accounting for less stabilization due to the increase of the strain energy. Such conformations were in agreement with NMR data, indicating a fast exchanging conformational flexibility between hydrogen-bonded structures. The global minimum conformer for compound **2** showed a kinked structure stabilized by a hydrogen bond between Asp NH and the carbonyl group of Gly, in agreement with NMR data (Fig. 4, bottom).

The results from the conformational analysis were consistent with IC₅₀ values, suggesting a close connection between the conformation and the ligand binding affinity, as compound **1**, having

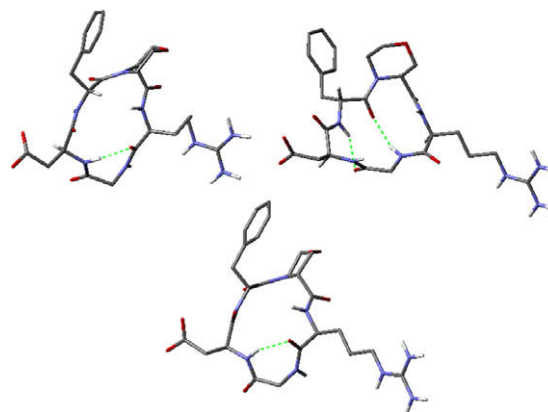


Figure 4. Energy-minimized conformations for **1** and **2**: top left: **1**, global minimum conformer; top right: **1**, 2nd low-energy conformer; bottom: **2**, global minimum conformer.

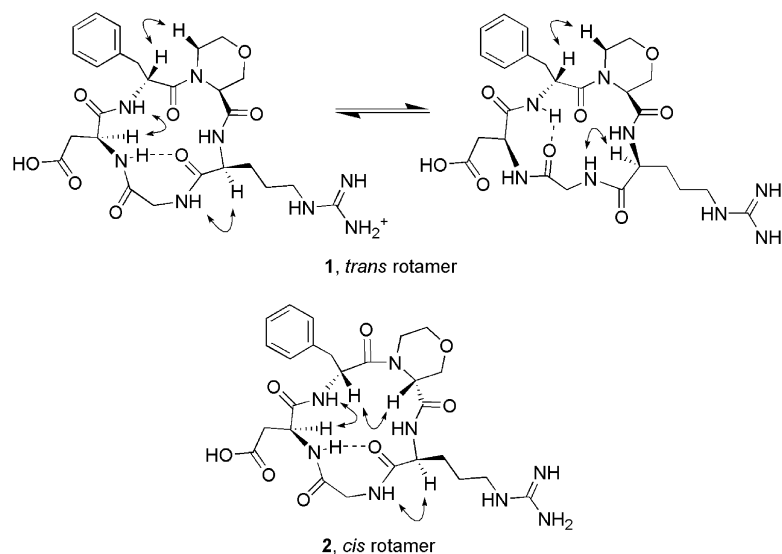


Figure 3. Selected ROESY peaks for compounds **1** (top) and **2** (bottom).

a more flexible structure, as a consequence of fast equilibration between two main conformations, resulted in a significantly lower binding capability than cyclopeptide **2**. Also, all experimental data suggested that the role of D-Mor in nucleating the correct conformation was due to the existence of the *cis*-rotamer, which allowed maintaining the required torsional angles between D-Phe and Arg for a good binding to the integrin. Finally, similar binding affinity for $\alpha_v\beta_5$ in both cyclopeptides **1** and **2** indicated such integrin to better accommodate both ligands, as a consequence of less stringent binding requirements compared to $\alpha_v\beta_3$.

2.4. Docking calculations

A docking simulation was carried using both ligands **1** and **2** with the aim to gain further insight into the possible binding modes of the cyclopeptides to the $\alpha_v\beta_3$ receptor at the molecular level. The crystal structure of the complex formed by c[RGDf(Me)V], and the extracellular fragment of the $\alpha_v\beta_3$ receptor (PDB code: 1L5G) provide a general mode of interaction between the integrin and its ligands.¹⁹ Specifically, the Asp carboxylate and the Arg guanidinium moiety of RGD-based ligands are the two key structural elements for the receptor recognition. In fact, the carboxylate group interacts with the metal ion dependant adhesion site (MIDAS) consisting of Mn^{2+} ions and Ser121/Ser123, whereas the Arg guanidinium group is responsible for salt bridge interactions with the side chains of Asp218 and Asp150. Also, additional ligand–receptor contacts engage Tyr122 in hydrophobic π -stacking and Asn215 in hydrogen-bonding interactions. The docking program Autodock 4.0.1²⁵ was used to evaluate the binding energies of selected conformations of **1** and **2** as potential ligands for the $\alpha_v\beta_3$ receptor, and the docked conformations were analysed taking into account the binding interactions observed in the crystal structure of the bound ligand–protein complex. The docking results for both ligands revealed the key interactions with Asp218 and the MIDAS site of the receptor, suggesting all these interactions to be necessary for the molecular recognition of the Arg–Gly–Asp-containing ligands, although they could not provide a criterion for determining their differences in affinity (Fig. 5). Specifically, the global minimum conformer of peptide **1**, conformer A, showed the Asp side chain located in the MIDAS site interacting with Ser121, and the guanidinium group of Arg experiencing only a monodentate interaction with Asp218 (Fig. 5, top). The same interactions were observed for the second low-energy conformation of **1**, conformer B (Fig. 5, middle), also displaying the benzyl group in the proximity of Tyr122 side chain, although the backbone structure was positioned in the shallow pocket between these two in a way considerably different from low-nanomolar RGD-based inhibitors, such as c[RGDf(Me)V], which is able to lay flatter and thus in closer contact with the protein surface.¹⁹ Peptide **2** resulted in a main cluster of conformations displaying the typical binding mode of RGD cyclopeptide-based ligands. Specifically, the cluster showed the canonical binding mode consisting in bidentate Asp218/Arg and MIDAS/Ser121/Asp interactions, and a hydrophobic π -stacking between D-Phe and Tyr122 (Fig. 5, bottom).

The comparison of the binding mode of compound **2** with respect to the reference ligand c[RGDf(Me)V], known also as EMD121974 (see Table 1), revealed some interesting issues to address the different bioactivity of the two ligands (Fig. 6). Although showing a similar binding mode of Asp and Arg side chains in the key region of the receptor (see Fig. 5), the two cyclopeptides showed a different conformation of the cyclopeptidic backbone. The reference ligand c[RGDf(Me)V] showed secondary interactions as a consequence of a different conformation exposing the Asp NH toward the receptor's cavity. Such proton established additional hydrogen-bonding interactions with either carbonyl groups of Asn215 or Arg216. Also, the guanidine group showed a bridged ori-

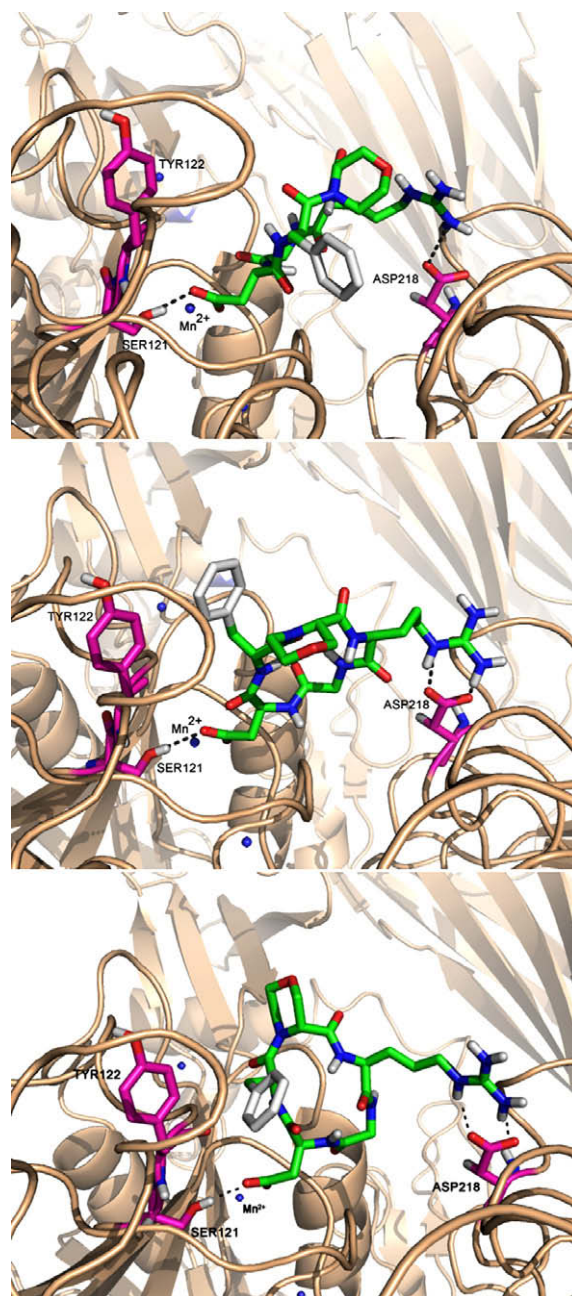


Figure 5. RGD ligands **1** and **2** (green) docked into the binding region of $\alpha_v\beta_3$ integrin highlighting the protein residues (magenta) that form the key interactions. Top: **1**, conformer A: Asp218 versus Arg, Ser121 and Mn^{2+} versus Asp; middle: **1**, conformer B: Asp218 versus Arg, Ser121 and Mn^{2+} versus Asp, Tyr122 versus D-Phe; bottom: **2**, Asp218 versus Arg, Ser121 and Mn^{2+} versus Asp, Tyr122 versus D-Phe. Non-polar hydrogen atoms are omitted for clarity.

entation between Asp218 and Asp150, although such interaction was also observed in some docked conformations of compound **2** (figure not shown). These differences in secondary interactions with integrins may explain the different binding affinity between the two ligands, especially towards $\alpha_v\beta_5$ integrin, where c[RGDf(Me)V] was found to be more active by two orders of magnitude with respect to compound **2**.

More interestingly, the prediction of the free energy of binding and of the corresponding K_i for the lowest-energy clusters of both compounds was in agreement with bioassay data (Table 3). In fact, the cluster of compound **1**, conformer A showed a binding energy of -9.5 kcal/mol and a predicted K_i of 262 nM, whereas the second

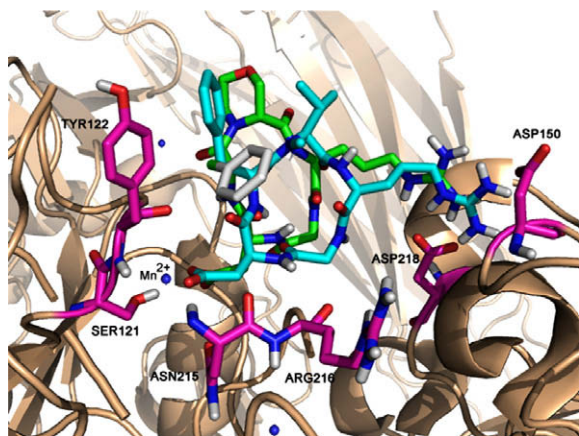


Figure 6. Overlap between the reference ligand c[RGDf(Me)V] (cyan), and compound **2** (green) in the binding region of $\alpha_v\beta_3$ integrin.

Table 3
Binding energy and predicted K_i values^a

Compound	Estimated free energy of binding (kcal/mol)	K_i (nM)
1A	−9.5	262
1B	−8.1	1003
2	−10.8	43

^a Taken as mean values of the docked conformations of the main cluster for each structure.

conformer (conformer B) resulted in lower binding affinity with the receptor, displaying a value of -8.1 kcal/mol for the binding energy and of 1.0 μ M for the predicted K_i value. On the contrary, the low-energy cluster of compound **2** showed a stronger affinity towards $\alpha_v\beta_3$, as demonstrated by the lower binding energy (-10.8 kcal/mol, see Table 3) and a predicted K_i value falling in the low nanomolar range.

3. Conclusion

We reported the synthesis of two cyclopentapeptides and the biological assay towards $\alpha_v\beta_3/\alpha_v\beta_5$ integrins containing both enantiomers of Mor. The binding affinity revealed *D*-Mor-containing ligand as the more active towards $\alpha_v\beta_3$, whereas the two cyclopeptides showed the same affinity for the $\alpha_v\beta_5$ integrin, indicating a less strict conformational requirement for optimal binding to this protein. The result was particularly striking as the *D*-amino acid-containing ligand retained the activity towards $\alpha_v\beta_3$ integrin, irrespective of the change of configuration at the X position of common integrin ligands having the c[RGDfX] sequence. Conformational analysis suggested the two enantiomeric secondary amino acids to stabilize two different conformations, as a consequence of diverse rotamers nucleated at the *D*-Phe-Mor peptide bond. Specifically, *D*-Mor established a *cis* peptide bond, which provided a unique conformation resembling the conformation of c[RGDf(Me)V] found in the crystal structure reported by Arnaout and co-workers¹⁹ Such conformation was characterized by a kinked conformation stabilized by a hydrogen-bond involving Asp amide proton. Conversely, *L*-Mor nucleated a *trans* peptide bond with the *D*-Phe carboxylic function, thus inducing equilibrating conformations stabilized by weak equilibrating hydrogen-bonds, which caused the two pharmacophoric side chain to be exposed in a less favourable orientation for optimal binding to $\alpha_v\beta_3$ integrin. The rationale of the present study may suggest the possibility to use other six-membered ring secondary α -amino acids

having *D*-configuration at the α -carbon as tools to nucleate bioactive conformations in cyclopentapeptides of general formula c[RGDfX].

4. Experimental

4.1. Chemistry

H-Gly-2-Cl-Trt resin (1.1 mmol/g) was purchased from Fluka. Chromatographic separations were performed on silica gel (Kieselgel 60, Merck) using flash-column techniques; R_f values refer to TLC carried out on 25-mm silica gel plates (Merck F₂₅₄) with the same eluant as indicated for column chromatography. All the solid phase reactions were carried out on a shaker, using solvent of HPLC quality. ¹H NMR spectra were recorded with Varian Gemini and Mercury NMR spectrometers operating at 200 MHz and 400 MHz for the proton, respectively. Bromophenol Blue (BB) test was performed following this procedure: a few resin beads were put in a vial and suspended in 0.5 mL of DMF; two drops of a 1% solution of bromophenol blue in dimethylacetamide were added and the sample was observed. The BB test was considered to be positive (presence of free amino groups) when the resin beads turned blue immediately, and negative (absence of free amino groups) when the beads remained colourless. ESI-MS spectra were recorded by a PE SCIEX API 365 spectrometer. Compounds **1** and **2** were purified by Beckman-Gold HPLC system equipped with a reverse-phase column (Alltima C18 10 μ m, 250 \times 10 mm, Alltech) using H₂O/CH₃CN gradient eluant buffered with 0.1% TFA (flow = 2.5 mL/min, λ = 254 nm, gradient eluant: CH₃CN 10%/5 min, CH₃CN 10–90%/25 min). Analytical HPLC analyses were performed using a Dionex UltiMate 3000 system equipped with a reverse-phase column (Alltima C18 5 μ m, 250 \times 4.6 mm, Alltech) and the same gradient eluant as described above.

4.1.1. c[RGDf-(3S)-Carboxymorpholine] (**1**)

H-Gly-2-Cl-Trt resin (466 mg, 0.5 mmol) was used as the starting material. Fmoc-deprotections and the completion of each coupling reaction were assessed by performing a BB test. The coupling of the first amino acid was performed with a solution of *N*-Fmoc-Arg(Pbf)-OH (973 mg, 1.5 mmol, 3 equiv), HOBT (203 mg, 1.5 mmol, 3 equiv) in DMF (4 mL) and DIPC (236 μ L, 1.5 mmol, 3 equiv) was added dropwise at 0 $^{\circ}$ C. The resulting mixture was stirred for 10 min at this temperature and for further 10 min at room temperature, then added to the resin. This mixture was shaken at room temperature overnight. The solution was drained and the resin was washed with 5% DIPEA in DMF (3 \times 5 mL) and DMF (5 \times 5 mL). Fmoc deprotection was performed with 30% piperidine in DMF (10 mL) for 30 min, followed by resin washings with DMF (3 \times 10 mL). After deprotection, H-Arg(Pbf)-Gly-2-Cl-Trt resin was suspended in a solution of TBTU (318 mg, 1 mmol, 2 equiv), *N*-Fmoc-(*S*)-morpholine-3-carboxylic acid (350 mg, 1 mmol, 2 equiv) and DIPEA (169 μ L, 1 mmol, 2 equiv) in DMF (3 mL) and shaken for two days. The solution was drained and the resin was washed with 5% DIPEA in DMF (3 \times 5 mL) and DMF (5 \times 5 mL). After deprotection, H-(3S)-carboxymorpholine-Arg(Pbf)-Gly-2-Cl-Trt resin was suspended in a solution of HOBT (203 mg, 1.5 mmol, 3 equiv), DIPC (236 μ L, 1.5 mmol, 3 equiv), *N*-Fmoc-*D*-Phe-OH (581 mg, 1.5 mmol, 3 equiv) in DMF (4 mL) and shaken overnight. The solution was drained and the resin was washed with 5% DIPEA in DMF (3 \times 5 mL) and DMF (5 \times 5 mL). After deprotection, H-*D*-Phe-(3S)-carboxymorpholine-Arg(Pbf)-Gly-2-Cl-Trt resin was suspended in a solution of TBTU (640 mg, 2 mmol, 4 equiv), *N*-Fmoc-Asp(*t*-Bu)-OH (825 mg, 2 mmol, 4 equiv) and DIPEA (342 μ L, 2 mmol, 4 equiv) in DMF (4 mL) and shaken for two days. The solution was drained and the resin was washed with 5% DIPEA

in DMF (3 × 5 mL) and DMF (5 × 5 mL). *N*-Fmoc-Asp(*t*-Bu)-*D*-Phe-(3*S*)-carboxymorpholine-Arg(Pbf)-Gly-2-Cl-Trt resin was finally deprotected and washed with DMF (5 × 5 mL) and DCM (5 × 5 mL). In a solid phase reaction vessel H-Asp(*t*-Bu)-*D*-Phe-(3*S*)-carboxymorpholine-Arg(Pbf)-Gly-2-Cl-Trt resin was treated with 5 mL of 1% TFA/DCM solution (10 × 2 min). The filtrates were immediately neutralized with a 10% pyridine/MeOH solution (1 mL), then the resin was washed with DCM (3 × 5 mL). The fractions containing the product (TLC:DCM/MeOH 4:1) were combined and concentrated under reduced pressure to yield a residue, which was suspended in H₂O and purified from the pyridinium salts by size-exclusion chromatography (AMBERLITE XAD2 resin, H₂O then MeOH). Evaporation of the combined MeOH fractions containing the product afforded the side-chain protected peptide (450 mg, 98%) as a white solid. The linear peptide (450 mg, 0.492 mmol) was dissolved under a nitrogen atmosphere in DMF (110 mL), then TBTU (474 mg, 1.47 mmol) and DIPEA (252 μL, 1.47 mmol) were added and the resulting mixture was stirred for 24 h at room temperature. The solvent was distilled under reduced pressure and the residue was dissolved in H₂O (60 mL) and extracted with EtOAc (3 × 80 mL); the organic phase was washed twice with 5% NaHCO₃, dried with Na₂SO₄ and evaporated under reduced pressure. The crude residue was purified by flash column chromatography (DCM/MeOH 9:1, *R*_f = 0.37) to afford the protected cyclic peptide (200 mg, 45%), as a white solid. HPLC: *t*_R = 23.80, purity: 86%. Side chain protected cyclic peptide (200 mg, 0.22 mmol), was treated with 95:2.5:2.5 TFA/H₂O/TIS mixture (20 mL) for 2 h. The reaction mixture was evaporated under reduced pressure and the residue was dissolved in H₂O (60 mL). The aqueous phase was washed with *i*Pr₂O (3 × 60 mL) and freeze-dried. The crude residue was purified by semi-preparative HPLC to give the side-chain deprotected **1** (38 mg, 13%), as a white solid. Trifluoroacetate ion was replaced with chloride ion by ion-exchange chromatography (AMBERLITE IRA-96 resin, chloride form). ESI-MS: (*m/z*) 589.2 [*M*⁺+H, 100]. HPLC: *t*_R = 13.8, purity 90%. See Table 4 for ¹H and ¹³C NMR data.

4.1.2. c[RGDF-(3R)-Carboxymorpholine] (2)

Compound **2** was prepared following the procedure as for **1**, using the scaffold *N*-Fmoc-(*R*)-morpholine-3-carboxylic acid. Cleavage from the solid support afforded the linear protected peptide in 83% yield, as a white solid. Cyclization using TBTU methodology afforded the protected cyclic peptide in 64% yield, as a white solid. HPLC: *t*_R = 22.8 (purity: 85%). Final deprotection in analogy with **1** afforded **2** as a white solid (40 mg, 14%). ESI-MS: (*m/z*) 589.2 [*M*⁺+H, 100], 611.1 [*M*⁺+Na, 7]. HPLC: *t*_R = 13.5, purity: 93%. See Table 4 for ¹H and ¹³C NMR data.

Table 4
¹H and ¹³C chemical shifts of **1** and **2** in DMSO-*d*₆ solutions at 298 K

	1 δ (ppm)		2 δ (ppm)	
	¹ H	¹³ C	¹ H	¹³ C
H-2	4.16, 3.45	66.9	4.26, 3.09	68.8
H-3	4.69	53.6	4.80	53.8
H-5	4.14, 3.43	67.0	2.84, 3.66	66.7
H-6	3.60, 3.12	65.9	3.33, 3.86	68.1
Gly NH	8.70	—	8.60	—
Arg NH	6.48	—	8.06	—
Asp NH	8.39	—	7.56	—
<i>D</i> -Phe NH	7.49	—	8.80	—
Gly H-α	3.79, 3.62	44.8	3.86–3.25	44.4
Arg H-α	4.53	53.5	3.96	53.5
Arg H-β,γ	2.02–1.91	26.8, 24.9	1.68–1.55	26.9, 25.0
Arg H-δ	3.11	40.0	3.11–2.98	40.7
Asp H-α	4.18	49.3	4.55	57.1
Asp H-β	2.66, 2.14	38.1	2.45–2.26	39.7
<i>D</i> -Phe H-α	5.02	50.4	4.82	50.3
<i>D</i> -Phe H-β	3.03, 2.68	37.9	3.08–2.73	38.2

4.2. Biology

4.2.1. Solid-phase receptor binding assay

[¹²⁵I]-Echistatin, labelled by the lactoperoxidase method²⁶ to a specific activity of 2000 Ci/mmol, was purchased from GE Healthcare. Integrin proteins α_vβ₃ and α_vβ₅ purified from human placenta were purchased from Chemicon International Inc, Temecula, CA. The receptor binding assay was performed as described.^{13,4b} Purified receptors α_vβ₃ and α_vβ₅ were diluted respectively at 500 ng/mL and 1000 ng/mL in coating buffer (20 mM Tris (pH 7.4), 150 mM NaCl, 2 mM CaCl₂, 1 mM MgCl₂, 1 mM MnCl₂). An aliquot of the diluted receptors (100 μL/well) was added to a 96-well microtiter plate (Optiplate-96 HB, PerkinElmer Life Sciences, Boston, MA) and incubated overnight at 4 °C. The plate was washed once with blocking/binding buffer (20 mM Tris (pH 7.4), 150 mM NaCl, 2 mM CaCl₂, 1 mM MgCl₂, 1 mM MnCl₂, 1% BSA) and incubated for additional 2 h at room temperature. The plate was rinsed twice with the same buffer, then competition binding studies were performed with a fixed concentration of [¹²⁵I]-Echistatin (0.05 nM and 0.1 nM for α_vβ₃ and α_vβ₅, respectively) and concentrations ranging from 0.01 nM and 100 μM of the tested compounds. All assays were performed in triplicate in a final volume of 0.2 mL, each containing the following species: 0.05 mL of [¹²⁵I]-Echistatin, 0.04 mL of the tested compound and 0.11 mL of blocking/binding buffer. Non-specific binding was defined as [¹²⁵I]-Echistatin bound in the presence of an excess (1 μM) of unlabelled echistatin. After incubation for 3 h at room temperature, the plate was washed three times with blocking/binding buffer, then counted in a Top-Count NXT microplate scintillation counter (PerkinElmer Life Sciences, Boston, MA) using 200 μL/well of MicroScint-40 liquid scintillation (PerkinElmer Life Sciences, Boston, MA).

4.2.2. Data analysis

The IC₅₀ values were determined by fitting binding inhibition data by non-linear regression using GraphPad Prism 4.0 Software Package (GraphPad Prism, San Diego, CA). Moreover, when the Hill slope of the curves was significantly less the unity (*K* < −0.80), the data were reanalysed with a two-site model. The displacement curves better fitted (*p* < 0.05) by a two-sites model than one-site model were considered significant.

4.3. NMR methods

NMR experiments were performed at a temperature of 298 K on Varian Inova and Varian Mercury 400 MHz NMR spectrometers using diluted DMSO-*d*₆ solutions. All proton chemical shifts were assigned unambiguously for **1** and **2**. Variable temperature 1D, and 2D experiments (TOCSY, gCOSY, ROESY, HSQC) were carried out at the sample concentration of 9.2 mM for **1** and 6.2 mM for **2**. One-dimensional ¹H NMR spectra for determining temperature coefficients were obtained at 298–323 K with increments of 5 K. Sample temperatures were controlled with the variable-temperature unit of the instrument. Proton signals were assigned via TOCSY spectra, and ROESY spectra provided the data used in the conformational analyses. TOCSY spectra were recorded with 2048 points in *t*₁, 256 points in *t*₂, and 8 scans per *t*₂ increment and using a mixing time of 80 ms. ROESY spectra were recorded with a similar number of *t*₁ and *t*₂ points unless otherwise noted, and 32 per *t*₂ increment, and using a mixing time of 0.5 s. ¹H and ¹³C chemical shifts of **1** and **2** are reported in Table 4.

4.4. Molecular modelling

Conformational preferences of compounds **1** and **2** were investigated by molecular mechanics calculations within the framework of MacroModel v6.5,^[21] using Amber^{*22} as a force field and the

implicit water GB/SA solvation model of Still et al.²³ Monte Carlo energy minimization (MCEM)²⁴ conformational searches of the peptide analogues containing methyl groups instead of the Arg and Asp side chains were performed as the first step. Selected ROE-cross peaks from ROESY spectra were taken into account for defining distance constraints. The torsional space of each AGA cyclopeptide was randomly varied with the usage-directed Monte Carlo conformational search. Ring-closure bonds were defined in the morpholine ring and in the cyclopeptide ring. Amide bonds were included among the rotatable bonds. For each search, at least 1000 starting structures for each variable torsion angle were generated and minimized until the gradient was less than 0.05 kJ/Å mol using the truncated Newton-Raphson method implemented in MacroModel. Duplicate conformations and those with an energy greater than 6 kcal/mol above the global minimum were discarded.

4.5. Docking calculations

Automated docking studies were carried out by the Autodock 4.0.1 program,²⁵ using the Lamarckian Genetic Algorithm (LGA) as a search engine. The AutoDockTools 1.4.5 (ADT) graphical interface²⁷ was used to prepare the receptor and the ligands PDBQT files. The coordinates of the ligands **1** and **2** were retrieved from the lowest energy conformers resulting from calculation using NMR data, whereas the coordinates of $\alpha_v\beta_3$ receptor was retrieved from the Protein Data Bank (PDB code: 1L5G), and the ligand–protein complex was unmerged for achieving free receptor structure. Water molecules were removed. For the protein receptor and ligands **1** and **2**, all hydrogens were added, Gasteiger charges were computed, and non-polar hydrogens were merged. A charge value of +2.0 to each Mn atom of the protein receptor was successively added. Three-dimensional energy scoring grids of 0.375 Å resolution and 40 Å × 40 Å × 40 Å dimensions were computed. The center of the grid was set to be coincident with the mass center of the ligands preliminary fitted on the X-ray structure of c[RGDf(Me)V] in the $\alpha_v\beta_3$ complex (1L5G). A total of 50 runs with a maximum of 2,500,000 energy evaluations were carried out for each ligand, using the default parameters for LGA. Cluster analysis was performed on the docked results using a root-mean-square (rms) tolerance of 1.5 Å. The analysis of the binding mode, the calculation of the binding energy and the prediction of the binding activity of the docked conformations were carried out using PyMol Autodock Tools plugin within PyMol software.²⁸

Acknowledgements

University of Florence, CINMPIS and MIUR are acknowledged for financial support. Dr. Filippo Sladojevich is acknowledged for carrying out preliminary synthetic experiments. Ente Cassa di Risparmio is acknowledged for the granting the 400 MHz NMR spectrometers.

References and notes

- (a) Arnaout, M. A.; Goodman, S. L.; Xiong, J. P. *Curr. Opin. Cell Biol.* **2002**, *14*, 641; (b) Hynes, R. O. *Cell* **2002**, *110*, 673; (c) Plow, E. F.; Haas, T. A.; Zhang, L.; Loftus, J.; Smith, J. W. *J. Biol. Chem.* **2000**, *275*, 21785; (d) Humphries, M. J. *Biochem. Soc. Trans.* **2000**, *28*, 311.

- Ruoslathi, E.; Pierschbacher, M. D. *Science* **1987**, *238*, 491.
- For $\alpha_v\beta_3$, see: (a) Eliceiri, B. P.; Cheresch, D. A. *Cancer J.* **2000**, *13*, 245; (b) Burke, P. A.; De Nardo, S. J.; Miars, L. A.; Lamborn, K. L.; Matzku, S.; De Nardo, G. L. *Cancer Res.* **2002**, *62*, 4263; (c) Haubner, R.; Finsinger, D.; Kessler, H. *Angew. Chem., Int. Ed.* **1997**, *36*, 1374; For $\alpha_v\beta_5$, see: (d) Marinelli, L.; Gottschalk, K. E.; Meyer, A.; Novellino, E.; Kessler, H. *J. Med. Chem.* **2004**, *47*, 4166; (e) Friedlander, M.; Theesfeld, C. L.; Sugita, M.; Fruttiger, M.; Thomas, M. A.; Chang, S.; Cheresch, D. A. *Proc. Natl. Acad. Sci.* **1996**, *93*, 9764; (f) Friedlander, M.; Brooks, P. C.; Shaffer, R. W.; Kincaid, C. M.; Varner, J. A.; Cheresch, D. A. *Science* **1995**, *270*, 1500.
- (a) Brooks, P. C.; Stromblad, S.; Klemke, R.; Visscher, D.; Sarkar, F. H.; Cheresch, D. A. *J. Clin. Invest.* **1995**, *96*, 1815; (b) Kumar, C. C.; Malkowski, M.; Yin, Z.; Tanghetti, E.; Yaremko, B.; Nechuta, T.; Varner, J.; Liu, M.; Smith, E. M.; Neustadt, B.; Presta, M.; Armstrong, L. *Cancer Res.* **2001**, *61*, 2232.
- Mitjans, F.; Meyer, T.; Fittschen, C.; Goodman, S.; Jonczyk, A.; Marshall, J. F.; Reyes, G.; Piulats, J. *Int. J. Cancer* **2000**, *87*, 716.
- MacDonald, T. J.; Taga, T.; Shimada, H.; Tabrizi, P.; Zlokovic, B. V.; Cheresch, D. A.; Laug, W. E. *Neurosurgery* **2001**, *48*, 151.
- Wermuth, J.; Goodman, S. L.; Jonczyk, A.; Kessler, H. *J. Am. Chem. Soc.* **1997**, *119*, 1328.
- (a) Bach, A. C.; Il; Espina, J. R.; Jackson, S. A.; Stouten, P. F. W.; Duke, J. L.; Mousa, S. A.; DeGrado, W. F. *J. Am. Chem. Soc.* **1996**, *118*, 293; (b) Dechantsreiter, M.; Plnaker, E.; Mathä, B.; Lohof, E.; Hölzemann, G.; Jonczyk, A.; Goodman, S. L.; Kessler, H. *J. Med. Chem.* **1999**, *42*, 3033; (c) Lohof, E.; Plnaker, E.; Mang, C.; Burkhardt, F.; Dechantsreiter, M. A.; Haubner, R.; Wester, H. J.; Schwaiger, M.; Hölzemann, G.; Goodman, S. L.; Kessler, H. *Angew. Chem. Int. Ed.* **2000**, *39*, 2761; (d) Belvisi, L.; Bernardi, A.; Checchia, A.; Manzoni, L.; Potenza, D.; Scolastico, C.; Castorina, M.; Capelli, A.; Giannini, G.; Carminati, P.; Pisano, C. *Org. Lett.* **2001**, *3*, 1001; (e) Casiraghi, G.; Rassa, G.; Auzzas, L.; Bureddu, P.; Gaetani, E.; Battistini, L.; Zanardi, F.; Curti, C.; Nicastro, G.; Belvisi, L.; Motto, I.; Castorina, M.; Giannini, G.; Pisano, C. *J. Med. Chem.* **2005**, *48*, 7675; (f) Belvisi, L.; Bernardi, A.; Colombo, M.; Manzoni, L.; Potenza, D.; Scolastico, C.; Giannini, G.; Marcellini, M.; Riccioni, T.; Castorina, M.; LoGiudice, P.; Carminati, P.; Pisano, C. *Bioorg. Med. Chem.* **2006**, *14*, 169.
- (a) Trabocchi, A.; Menchi, G.; Guarna, F.; Machetti, F.; Scarpi, D.; Guarna, A. *Synlett* **2006**, 331; (b) Trabocchi, A.; Potenza, D.; Guarna, A. *Eur. J. Org. Chem.* **2004**, 4621; (c) Trabocchi, A.; Occhiato, E. G.; Potenza, D.; Guarna, A. *J. Org. Chem.* **2002**, *67*, 7483.
- Sladojevich, F.; Trabocchi, A.; Guarna, A. *J. Org. Chem.* **2007**, *72*, 4254.
- Krchnák, V.; Vágnér, J.; Sáfár, P.; Lebl, M. *Collect. Czech. Chem. Commun.* **1988**, *53*, 2542.
- Belkin, V. M.; Belkin, A. M.; Koteliansky, V. E. *J. Cell Biol.* **1990**, *111*, 2159.
- Pytela, R.; Pierschbacher, M. D.; Argraves, S.; Suzuki, S.; Ruoslahti, E. *Methods Enzymol.* **1987**, *144*, 475.
- Kumar, C. C.; Nie, H.; Rogers, C. P.; Malkowski, M.; Maxwell, E.; Catino, J. J.; Armstrong, L. *J. Pharmacol. Exp. Ther.* **1997**, *283*, 843.
- (a) Dijkgraaf, I.; Kruijtz, J. A.; Frielink, C.; Soede, A. C.; Hilbers, H. W.; Oyen, W. J.; Corstens, F. H.; Liskamp, R. M.; Boerman, O. C. *Nucl. Med. Biol.* **2006**, *33*, 953; (b) Zanardi, F.; Burreddu, P.; Rassa, G.; Auzzas, L.; Battistini, L.; Curti, C.; Sartori, A.; Nicastro, G.; Menchi, G.; Cini, N.; Bottoncetti, A.; Raspanti, S.; Casiraghi, G. *J. Med. Chem.* **2008**, *51*, 1771.
- Takagi, J.; Petre, B. M.; Walz, T.; Springer, T. A. *Cell* **2002**, *110*, 599.
- Humphries, M. J.; McEwan, P. A.; Barton, S. J.; Buckley, P. A.; Bella, J.; Mould, A. P. *Trends Biochem. Sci.* **2003**, *28*, 313.
- Shimaoka, M.; Springer, T. A. *Nat. Rev. Drug Discov.* **2003**, *2*, 703.
- Xiong, J. P.; Stehle, T.; Zhang, R.; Joachimiak, A.; Frech, M.; Goodman, S. L.; Arnaout, M. A. *Science* **2002**, *296*, 151.
- Bednar, R. A.; Gaul, S. L.; Hamill, T. G.; Egbertson, M. S.; Shafer, J. A.; Hartman, G. D.; Gould, R. J.; Bednar, B. J. *Pharmacol. Exp. Ther.* **1998**, *285*, 1317.
- Mohamadi, F.; Richards, N. G. J.; Guida, W. C.; Liskamp, R.; Lipton, M.; Caufield, C.; Chang, G.; Hendrickson, T.; Still, W. C. *J. Comput. Chem.* **1990**, *11*, 440.
- Weiner, S. J.; Kollman, P. A.; Nguyen, D. T.; Case, D. A. *J. Comput. Chem.* **1986**, *7*, 230.
- Still, W. C.; Tempczyk, A.; Hawley, R. C.; Hendrickson, T. *J. Am. Chem. Soc.* **1990**, *112*, 6127.
- Chang, G.; Guida, W. C.; Still, W. C. *J. Am. Chem. Soc.* **1989**, *111*, 4379.
- Morris, G. M.; Goodsell, D. S.; Halliday, R. S.; Huey, R.; Hart, W. E.; Belew, R. K.; Olson, A. J. *J. Comput. Chem.* **1998**, *19*, 1639.
- Kumar, C. C.; Nie, H.; Armstrong, L.; Zhang, R.; Vijay-Kumar, S.; Tsarbopoulos, A. *FEBS Lett.* **1998**, *429*, 239.
- Gillet, A.; Sanner, M.; Stoffer, D.; Olson, D. *Structure* **2005**, *13*, 483.
- DeLano, W. L. The PyMOL Molecular Graphics System, DeLano Scientific LLC: San Carlos, CA, USA. <http://www.pymol.org>.